ELSEVIER

Available online at www.sciencedirect.com

SCIENCE DIRECT®

Polymer 46 (2005) 7176–7184

polymer

www.elsevier.com/locate/polymer

Control of fluorescence emission color of benzo 15-crown-5 ether substituted oligo phenylene vinylene–ceramic nanocomposites

G. Ramachandran[a], G.P. Simon[a,*], Y.B. Cheng[a], L. Dai[b]

[a]*Department of Materials Engineering, Monash University, Wellington Rd, Clayton, Vic. 3800, Australia*
[b]*Department of Polymer Engineering, University of Akron, Akron, OH 44325-2909, USA*

Received 28 January 2005; accepted 17 May 2005
Available online 1 July 2005

Abstract

Nanocomposites of benzo 15-crown-5 ether substituted oligo phenylene vinylene (CE–OPV) were prepared by solution intercalation into a surface treated bentone clay, B34, in both the presence and absence of Eu^{3+} ions, and were characterized using X-ray diffraction (XRD) and fluorescence techniques. The intercalation of B34 by CE-OPV increases the *d*-spacing (gallery height) of B34, the increase being more in the presence of metal ion than in its absence. The increase in *d*-spacing of a related material, poly[1,4,-(2,5-bis (tetra ethylene oxide substituted)) phenylene vinylene (EO-PPV)] due to intercalation into clay is greater than that by CE-OPV. Results on intercalation of small benzo-crown ether molecules themselves into B34 in the presence and absence of Eu^{3+}, are also presented to help elucidate the process. The fluorescence emission maxima of the nanocomposites of CE-OPV, CE-OPV-Eu^{3+} and EO-PPV showed a steady blue shift as a function of B34 composition and the results are explained in terms of partial intercalation of the fluorophores into the clay.

Keywords: Fluorescence; Nanocomposite; Crown ether

1. Introduction

There is growing interest in research utilizing poly(para phenylene vinylenes) (PPV) as active elements of light emitting diodes (LED) [1], plastic lasers [2,3] photovoltaic devices [4], light emitting electrochemical cells (LEC) [5, 6], field effect transistors [7], photo detectors [8] and photo diodes [9,10], emphasizing the importance of these materials in optoelectronic applications. One novel area of research with PPV materials involves orienting PPV molecules by their intercalation into molybdate [11], silicate [12], mesoporous silica [13,14], mica [15] and a lyotropic liquid crystal (LC) polymer [16,17]. We have previously reported a blue-shift in the fluorescence emission maximum of a related material, poly[1,4,-(2,5-bis(tetra ethylene oxide substituted)) phenylene vinylene] (EO-PPV) intercalated into an organically-modified clay, bentone 34 (B34), changing from 610 to 570 nm [12]. Similar blue shifts in fluorescence emission maximum of PPV in the nanocomposites of PPV-polymeric LC [16,17] were attributed to truncated conjugation of PPV segments in the composite [16] and aggregation of PPV excited states [17]. Conversely, intercalation of poly[2-methoxy-5-(2-ethyl) hexyloxy para phenylene vinylene] (MEH-PPV) into mica [15] and mesoporous silica [13,14] has shown a red-shift in photoluminescence emission maximum, ascribed to emission from the elongated polymeric segments oriented within the pore [13,14] and galleries [15]. Apart from PPV, other conjugated polymers which have been incorporated into clay particles are polyolefins [18], polyimides [19], polypyrrole [20] and polyaniline [21].

We have previously published work [22], that indicated that emission maxima of PPV material can be varied by addition of ions such as Eu^{3+} to modified PPV materials, due to the formation of complexes, thereby providing a method to manipulate fluorescence emission maxima. This paper represents first report of a fluorophore, a PPV oligomer and its metal ion being intercalated into a nanoclay. The oligomer of interest is benzo-15-crown-5 ether substituted oligo phenylene vinylene (CE-OPV) (Scheme 1) and the clay is a commercially available organically-modified clay. To study the effect of

---

* Corresponding author.
E-mail address: george.simon@eng.monash.edu.au (G.P. Simon).

0032-3861/$ - see front matter © 2005 Elsevier Ltd. All rights reserved.
doi:10.1016/j.polymer.2005.05.087

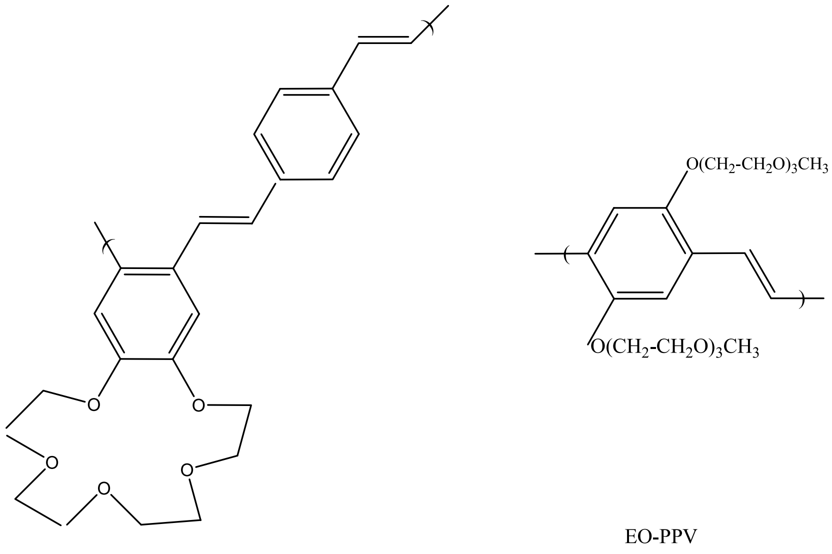

CEOPV

EO-PPV

Scheme 1. Structure of the two fluorophores used for intercalation into B34.

complexation on intercalation, we performed intercalation experiments of CE-OPV both in the presence and absence of Eu^{3+} ion. For a better understanding of interactions, intercalation of polymeric EO-PPV (Scheme 1) is also studied to determine the different effects between cyclic crown ether (CE) and linear ethylene oxide (EO) moiety, in terms of the degree of intercalation and photoluminescence. For similar reasons, low molecular weight crown ethers and Eu^{3+} ions were also intercalated alone into the clay.

2. Experiment

2.1. Characterization

Fluorescence spectra of the solid films of the nanocomposites were recorded on a Perkin–Elmer LS 50 spectrophotometer. Powder X-ray diffraction (XRD) was used to confirm the intercalation of the oligomer, polymer and small organic molecules into the gallery of the organically modified clay B34, using Rigaku goniometer (Cu Kα, $\lambda = 0.154$ nm).

2.2. Materials

The solvents, methanol (BDH) and chloroform (BDH) were of AR grade and used as received. Europium(III) chloride hexa hydrate ($EuCl_3 \cdot 6H_20$) (Aldrich), benzo-15-crown-5 ether (Aldrich) and sodium chloride (NaCl) (BDH) were also used. The organically-modified layered silicate clay, B34 (Rheox, USA) was used, where the bentonite galleries are occupied by organically-modified cations, dimethylditallow ammonium cations. The formula of dimethylditallow ammonium cations is $(CH_3)_2N^+(CH_3(CH_2)_{13,15,17})_2$ with $C_{14} \sim 5\%$, $C_{16} \sim 25\%$, and $C_{18} \sim 70\%$.

The oligomer CE-OPV (Scheme 1) and the polymer EO-PPV (Scheme 1) were synthesized using a previously reported method [23,24]. In our synthesis, the oligomer is soluble in methanol and acetone was used for precipitation and purification of the oligomer. Gel permeation chromatography result and NMR spectra were used to confirm the molecular structure and molecular weight [23]. Solid films cast from a methanol-based solution of CE-OPV, when excited at 370 nm, and show emission maximum at 516 nm which is close to the reported PL emission maximum for CE-OPV, 515 nm [23]. The polymer, EO-PPV has been synthesized according to the previously reported procedure [24].

2.3. Solution intercalation experiments

Due to the good solubility of CE-OPV, BCE and $EuCl_3$ in methanol, the solution intercalation method was chosen to prepare the nanocomposites. As EO-PPV is insoluble in methanol, chloroform solvent was used for intercalation, since it is soluble in this medium. The preparative methods for various components are detailed as follows.

2.3.1. Effect of solvent on B34

Both methanol and chloroform are the solvents employed in these studies and it was first necessary to study the effect of these solvents on *d*-spacing of B34. In this way it is intended to determine the degree to which changes in spacing of the clay layers are due to solvent capture, and retention after film formation and drying. For this purpose, 50 mg samples of B34 were mixed with varying amounts of solvents and stirred for 16 h, at room temperature. The resulting slurries were coated uniformly onto glass substrates for XRD measurements. The films on glass substrates are dried at room temperature, under a vacuum of 1 mmHg pressure for 120 min, immediately after coating.

Since any possible changes in gallery spacing of B34 may depend on solvent type and/or the amount of solvent, the ratio of B34/solvent (mg/ml) was kept constant for a given set of experiments. To ensure comparability, a blank experiment with B34 and solvent alone was always undertaken with the same ratio of B34-to-solvent, as for the other mixtures.

2.3.2. Intercalation of CE-OPV (benzo-crown-5 ether substituted oligo phenylene vinylene) without metal ion

For intercalation experiments in the absence of metal ions, appropriate amounts of standard solution of CE-OPV in methanol were added to accurately-weighed samples of B34, the weight ratio of CE-OPV /B34 varied from 10/90 to 60/40. The ratio of weight by volume of B34 in methanol is kept constant. All the samples thus prepared were stirred for 12 h at room temperature (20 °C). The samples were cast as thin films on glass plates for XRD measurements, and on quartz plates for fluorescence measurements. The films dried by evaporating the solvent under vacuum, at room temperature for, 1 h.

2.3.3. Intercalation of CE-OPV (benzo-crown-5 ether substituted oligo phenylene vinylene)-Eu^{3+} complex

In an earlier report, we presented the results on fluorescence enhancement of CE-OPV-Eu^{3+} complex in solution [22]. The fluorescence enhancement was maximum when the molar ratio of Eu^{3+} /CE-OPV was 10. Therefore, CE-OPV-Eu^{3+} complex with the molar ratio of metal ion to CE-OPV of 10 was chosen for this work, which is equivalent to the weight ratio of metal ion to CE-OPV being 9:1. For intercalation experiments, appropriate amounts of standard solution of CE-OPV-Eu^{3+} of weight ratio of 1:9 in methanol were added to accurately weighed B34 samples. The ratio of B34 to methanol was constant for all the samples. Mixing to encourage intercalation was carried out for 12 h and samples were prepared for XRD and fluorescence spectroscopy, in the same manner described above for samples without metal ion.

2.3.4. Intercalation of benzo-crown-5 ether (BCE) into B34

The intercalation of benzo-crown-5 ether into B34 was carried out in the same way as intercalation of CE-OPV into B34. Another set of experiments was carried out in the presence of Eu^{3+} ion and at the weight ratio Eu^{3+} to BCE of 1:1.

2.3.5. Direct comparison of CE-OPV (benzo-crown-5 ether substituted oligo phenylene vinylene) intercalation with EO-PPV intercalation

Chloroform was used as the solvent for solution intercalation of CE-OPV and EO-PPV, due to the solubility of EO-PPV in chloroform. The intercalations were carried out in the same manner as those using methanol as the solvent.

3. Results and discussion

3.1. XRD analysis

3.1.1. Effect of solvent on B34

Fig. 1 shows the XRD patterns of B34 as received powder, films cast from a chloroform mixture and films cast from a methanol mixture. It can be seen that the gallery height (*d*-spacing of 001 plane) of B34 film produced from a chloroform slurry (2.60 nm) is lower than that of fresh B34 powder (3.10 nm). However, the *d*-spacing does not vary as a function of ratio of B34/chloroform (mg/ml), when the slurries are subjected to same conditions of stirring, casting the films and drying conditions. When methanol is used as the solvent, the *d*-spacing increased slightly, depending on methanol concentration (2.36 nm for 50 mg B34/2 ml methanol to 3.21 nm for 50 mg B34/3 ml methanol).

The decrease in *d*-spacing of B34 in chloroform implies a slight loss of alkyl ammonium ions from the gallery of B34. Conversely, the increase in *d*-spacing in methanol can be attributed to the entrapment of methanol inside B34 gallery due to the favorable polar interaction of methanol with the surface of the bentonite clay and the alkyl ammonium ions of B34.

3.1.2. Intercalation of CE-OPV(benzo-crown-5 ether substituted oligo phenylene vinylene) and its Eu^{3+} complex into B34

Fig. 2 shows the traces, and Table 1 the results of intercalation of CE-OPV in the presence and in the absence of metal ion into B34. Methanol, being a better solvent for Eu^{3+} than chloroform, was used for the intercalation experiments in this section. In Fig. 2, CE-OPV, and Eu^{3+} samples on their own do not show any peaks in the XRD spectra. Fig. 2(f) (nanocomposites CE-OPV-B34) and Fig. 2(e) Eu^{3+}-B34 show peaks corresponding to the *d*-spacing of intercalated B34. In the absence of metal ion, the *d*-spacing increases from 3.21 nm for B34 film to 3.76 nm for the maximum 60% CE-OPV in B34 (Table 1). The increase in *d*-spacing as a function of CE-OPV indicates that CE-OPV intercalates into the gallery of B34. When metal ions and CE-OPV are both present in the system, the *d*-spacing increases from 3.21 nm for B34 film, to 4.21 nm for 60% (1:9 CE-OPV-Eu^{3+}) in B34, as per Table 1. However, Eu^{3+} ion alone intercalates into B34, causing an increase in *d*-spacing of B34 from 3.21 to 3.68 nm (Fig. 2(e)). Therefore, a greater increase in *d*-spacing with the intercalation of CE-OPV in the presence of metal ion can be attributed to the additional metal ion. From Table 1 it can be seen that the change in *d*-spacing due to (6% CE-OPV-B34) is very small and thus the 1 nm increase in *d*-spacing

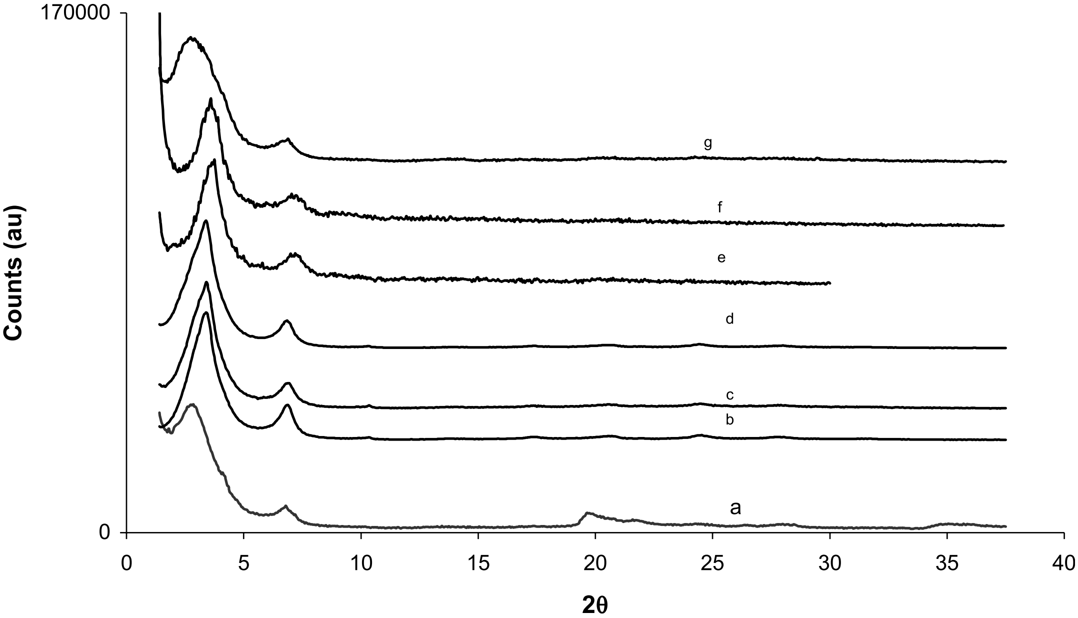

Fig. 1. XRD patterns for (a) B34 powder, and films made from the dispersions of 50 mg B34 in (b) 0.73 ml chloroform, (c) 1.6 ml chloroform, (d) 3 ml chloroform, (e) 2 ml methanol, (f) 2.5 ml methanol and (g) 3 ml methanol.

of the nanocomposite of 60%(1CE-OPV-9Eu^{3+}) is due to Eu^{3+} only. However, the increase in *d*-spacing due to 50% Eu^{3+} is just 0.47 nm, significantly lesser than 1 nm. Therefore, the increase in *d*-spacing of Eu^{3+}-CE-OPV-B34 nanocomposite (compared to that of CE-OPV-B34) is not merely due to additive effect of the two intercalating components, but is greater, most likely due to the combined, less-close-packed conformation of the polymer and ion together within the gallery.

3.1.3. Intercalation of CE-OPV (benzo-crown-5 ether substituted oligo phenylene vinylene) and EO-PPV poly[1,4,-(2,5-bis(1,4,7,10-tetra oxa undecyl) phenylene vinylene)

EO-PPV is a long chain polymer ($M_w = 22{,}000$ g/mol) [24] while CE-OPV is an oligomer ($M_w = 3600$ g/mol) [23]. The intercalation results of EO-PPV into B34 have been previously reported in the literature [12]. In order to compare the intercalation behavior of the oligomer and

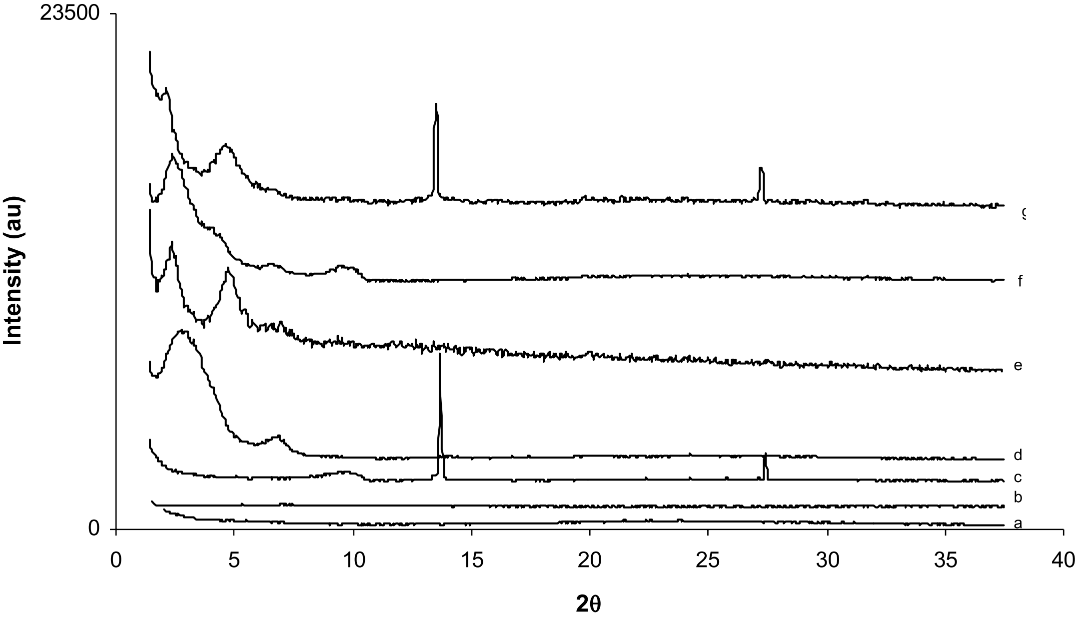

Fig. 2. XRD pattern for (a) CE-OPV, (b) $EuCl_3$, (c) (CE-OPV)-Eu complex of weight ratio 1:9, and films made from the dispersions of (d) 50 mg B34/3 ml methanol, (e) 50 mg B34 and 40 mg $EuCl_3$ in 3 ml methanol, (f) 50 mg of B34 and 50 mg CE-OPV in 3 ml methanol, and (g) 50 mg of B34 in a 3 ml methanol solution of 50 mg of 1:9 (CE-OPV)/$EuCl_3$ complex.

Table 1
Intercalation of CE-OPV into B34 in the presence and absence of metal ions, with B34/methanol being 50 mg/3 ml

No.	Un complexed CE-OPV				1:9 CE-OPV:Eu^{3+} metal complex				
	%CE-OPV	%B34	2θ (degree)	*d* (nm)	% Eu^{3+}	%CE-OPV	%B34	2θ (deg)	*d* (nm)
1	0	100	2.75	3.21	0	0	100	2.75	3.21
2	10	90	2.75	3.21	9	1	90	2.75	3.21
3	20	80	2.65	3.13	8	2	80	2.30	3.84
4	30	70	2.55	3.33	7	3	70	2.25	3.93
5	40	60	2.45	3.61	6	4	60	2.25	3.93
6	50	50	2.40	3.68	5	5	50	2.15	4.11
7	60	40	2.30	3.76	4	6	40	2.10	4.21
8	100	0	–	–	90	10	0	–	–

polymer with the different side groups (polyethylene oxide vs. crown ether) under identical conditions, intercalation experiments were carried out in chloroform. Fig. 3 shows the plot of *d*-spacing as a function of amounts of EO-PPV or CE-OPV in the nanocomposites. It can be seen that when the composition has 10% of EO-PPV or CE-OPV in B34 during intercalation reaction, the *d*-spacing is greater for EO-PPV composite (3.53 nm) than for the CE-OPV composite (2.72 nm). When the composition of EO-PPV or CE-OPV in B34 exceeds 30%, the *d*-spacing becomes almost identical for both CE-OPV and EO-PPV, as shown in Fig. 3.

The greater gallery expansion of EO-PPV at lower compositions, compared with that of CE-OPV in B34 may be either due to the high molecular weight of EO-PPV or due to more favorable interaction of long chain alkyl ammonium ion of B34 to the polyether functional groups of EO-PPV, compared to the crown ether groups of CE-OPV. The much reduced difference in *d*-spacing between EO-PPV and CE-OPV composites at higher compositions (>30% of EO-PPV or CE-OPV in B34) is proposed to occur due to the saturation of the gallery with the material, which seems to be determined by the clay and organo-ions, rather than by the precise structure of the ingressed polymer.

3.1.4. Intercalation of BCE (benzo-15-crown-5 ether) into B34

Although higher molecular weight polyethylene oxide has been reported to have been intercalated into B34 [26], intercalation of crown ether alone has not been reported, and is useful when trying to ascertain the effect these pendant units of PPV on intercalation. Following are the results of intercalation of crown ether alone into B34.

Fig. 4 shows that BCE can be intercalated into B34 by increasing *d*-spacing from 2.36 nm for B34 to 3.33 nm for 60% BCE in B34. The ratio of B34 to methanol in all these experiments were kept constant at 50 mg/2 ml. It can be seen that the intensities of the peaks due to intercalation of BCE at $2\theta = 9$, 17.5 and 27°, increase with an increase in the concentration of BCE in the nanocomposites (Fig. 4). This is clearly less than EO-PPV, not surprisingly the PPV polymer pushing the layers apart. Interestingly, comparison of the BCE-induced changes in *d*-spacing (0.97 nm) and poly(ethylene oxide) alone by solution intercalation [26] (0.36 nm) at high compositions, indicates that the bulky nature of the crown ether causes greater layer separation than ethylene oxide (indeed, the molecular weight of the poly(ethylene oxide) reported in Ref. [26] to cause the 0.36 nm change is 172,700 g/mol, significantly higher than the molecular weight of the ethylene oxide subsitutent on EO-PPV which is ca. 150 g/mol). (Note: by implication, polymeric poly(ethylene oxide)) causes considerably less *d*-spacing than either EO-PPV or CE-PPV—the rigid PPV chains that are energetically enticed into the galleries because of

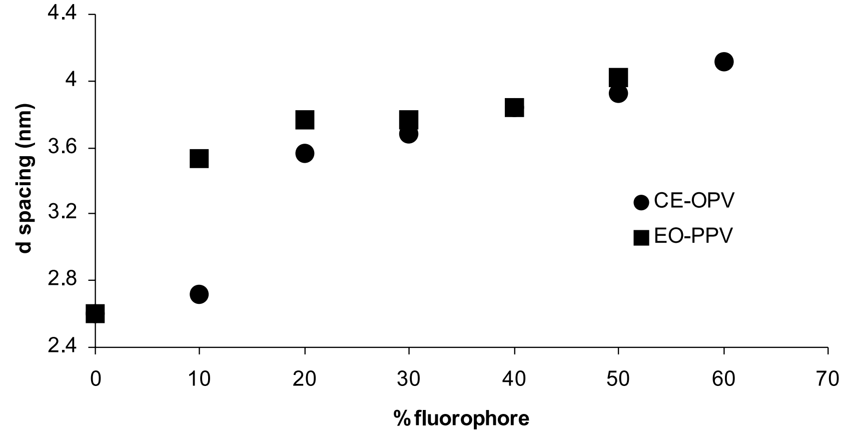

Fig. 3. Plot of *d*-spacing vs wt% fluorophore in the composites of B34 with EO-PPV and CE-OPV.

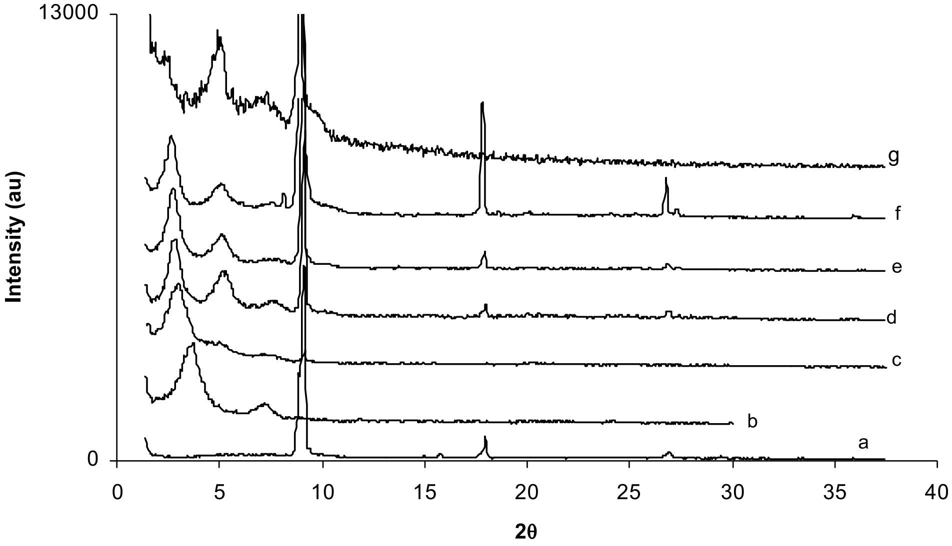

Fig. 4. XRD patterns for BCE-B34 nanocomposites of BCE/B34 ratio of (a) 100/0, (b) 0/100, (c) 10/90, (d) 30/70, (d) 50/50 and (e) 60/40 all with the ratio of 50 mg B34/2 ml methanol and (g) 1:1:1 BCE/$EuCl_3$/B34 with 40 mg B34 in 2 ml methanol.

their ethylene oxide or crown ether subsitutents, causes larger changes in *d*-spacing.

It can be seen in Fig. 4(g) and Table 2 that the complexation of BCE with Eu^{3+} causes the *d*-spacing to increase from 3.47 nm (for the nanocomposite with 1:1 weight ratio of B34:BCE) to 3.76 nm (for the nanocomposite in which the composition of B34:BCE:Eu^{3+} is 40:40:34 by weight). It should be noted that the *d*-spacing for the blank B34 and 1:1 B34:BCE are 2.45 and 3.47 nm, respectively. These values are higher than those observed in Fig. 4(a) (2.36 nm for B34 alone) and 4d (3.21 nm for 50% BCE in B34). It should be noted that the ratio of B34/methanol for the set of experiments in Table 2 is 40 mg/2 ml while that for the set of experiments for Fig. 4 is 50 mg/2 ml. The increase in methanol causes more of an increase overall in the *d*-spacing of B34 for the set of experiments for Table 2 than the experiments corresponding to Fig. 4.

When BCE alone is intercalated, an increase in *d*-spacing for B34 is 1.01 nm as per Table 2. With Eu^{3+} intercalation the increment in the *d*-spacing of B34 is 1.31 nm as per the same Table 2. This increase in B34 *d*-spacing due to Eu^{3+} is again more than the observed 0.47 nm increase due to Eu^{3+} intercalation inside B34 as reported in the earlier section of this report. Again, it should be noted that, this is due to the different ratio of B34/methanol used in these different sets of experiments. The calculated increase in *d*-spacing for Eu^{3+} and BCE is 2.32 nm as per data in Table 2, while the observed increment is 1.227 nm. This result indicates Eu^{3+} complexation induces a close packing of BCE inside the B34 gallery. This result is contrary to the intercalation of Eu^{3+}-(CE-OPV) discussed in the earlier part of this report, where Eu^{3+} complexation causes a less close packing of CE-OPV into B34. The presence of rigid vinyl bonds that connects the crown ether units of CE-OPV may prevent the oligomer to form a close packed complex with Eu^{3+}, while it is more possible with the system of individual crown ether units of BCE.

Table 2
Intercalation of BCE into B34 in the presence and in the absence of Eu^{3+} with B34/methanol ratio of 40 mg/2 ml

No.	Sample	Wt ratio in mg/2 ml methanol	*d*-spacing (nm)
1	B34	40	2.454
2	B34-BCE	40:40	3.465
3	B34-BCE-Eu	40:40:34	3.760
4	B34-Eu	40:34	3.681

3.2. Fluorescence

The results of the XRD experiments on CE-OPV and CE-OPV-Eu^{3+} discussed so far indicate that these materials can be intercalated into B34, the latter in a partial sense. The fluorescence spectra are of much interest, not only because the aim of the work is to manipulate the fluorescence emission by intercalation into clay, but also because of the interest in comparing the results with other recently-studied systems. The main related materials reported to date are MEH-PPV and EO-PPV. In the case of MEH-PPV intercalation, a red shift in fluorescence emission maximum was observed and ascribed to the fluorescence from completely intercalated MEH-PPV segments inside the gallery [13–15]. Winkler et al. reported a blue shift in fluorescence emission maximum of EO-PPV when intercalated into B34 [12] and explained this on the basis of completely intercalated EO-PPV inside the gallery. Therefore, it is of interest to determine the fluorescence emission maximum of nanocomposites of cyclic crown ether substituent in a PPV type material, compared to the linear ethylene oxide substituted PPVs.

The fluorescence spectra of the neat CE-OPPV and nanocomposites with 10–60% CE-OPV in B34 are shown in Fig. 5. It can be seen that there is a steady decrease in the fluorescence emission wavelength (blue-shift) as the clay concentration increases in the nanocomposites. The blue-shift is linear as a function of amount of clay in the nanocomposites as can be seen in Fig. 6(b). Similar kinds of blue-shift as a function of amount of clay are reported in the literature for EO-PPV intercalation into B34 [12]. Experiments using similar EO-PPV materials were repeated in this work, and the blue-shift in the emission maximum of EO-PPV upon intercalation in B34 was once again found, and is shown in Fig. 6(c). Fig. 6(a) shows a similar blue-shift in the fluorescence emission of CE-OPV-Eu^{3+}-B34 nanocomposite as a function of percentage of B34 in the nanocomposite.

To explain our results, we propose a model, as shown in Scheme 2. In it, the chains of CE-OPV or EO-PPV molecules are randomly oriented before intercalation. Upon intercalation the chains can be (a) completely intercalated (b) partially intercalated, and (c) unintercalated. As PPV type polymers emit visible radiation, fluorescence detection is readily possible for the partially intercalated segments of ‘b’ in Scheme 2, and completely unintercalated segments of ‘c’. In the completely intercalated nanocomposite ‘a’ of Scheme 2, fluorescence detection is only possible, if the detector of the instrument is exposed to the emitting radiation. This occurs only if the silicate layers of the composites are oriented parallel to the direction of emitting radiation and the molecules within the layers can be probed (‘seen’). In such an orientation, a red-shift is fluorescence emission would occur [13,14], due to the lower energy of the segments intercalated inside the gallery.

However, we observed a steady blue-shift, with the amount of B34 in the nanocomposites as shown in Fig. 6. As the amount of clay increases, it is possible for both the complete and partial intercalation to increase. In such a situation, when the silicate layers hide the emission of completely intercalated segments to the detector, only emission from the segments of partially-intercalated chains remaining outside the clay are detected. As the amount of clay increases, the intercalation will increase, resulting in a reduction in the amount of conjugated segments remaining outside the gallery. As emission maximum wavelength is directly related to the amount of conjugated segments [25], a systematic blue shift is observed with increasing amounts of clay in our system. This is clearly what is viewed in these systems with these treated clays, both for the CE-OPV and EO-PPV materials.

4. Conclusion

The conjugated oligomer CE-OPV and its complex with Eu^{3+} are solution intercalated into B34, to study the control of emission color as a function of intercalation. CE-OPV was intercalated into B34 in the presence and in the absence of metal ions, in methanol solution. The increase in *d*-spacing due to intercalation is greater in presence of Eu^{3+} than in its absence, because the metal ion alone can also intercalate into B34, causing an increase in *d*-spacing of the gallery. When intercalation is performed in chloroform, high molecular weight EO-PPV intercalates and causes a greater *d*-spacing change at lower concentrations of polymer than does low molecular weight CE-OPV, although this becomes greater at higher concentrations of additive

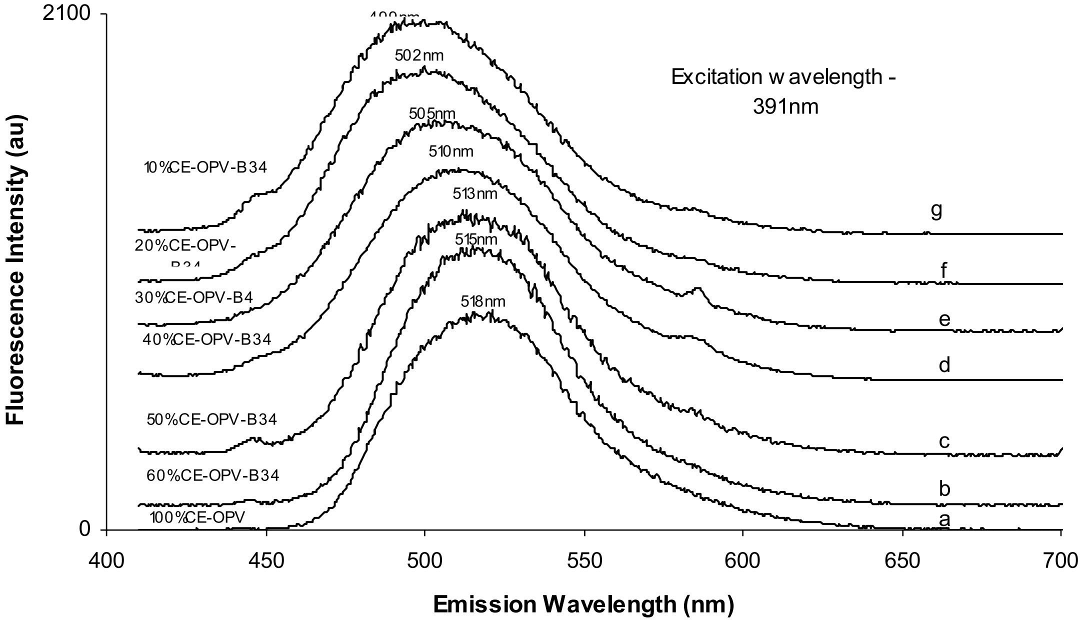

Fig. 5. Fluorescence spectra of CE-OPV-B34 films.

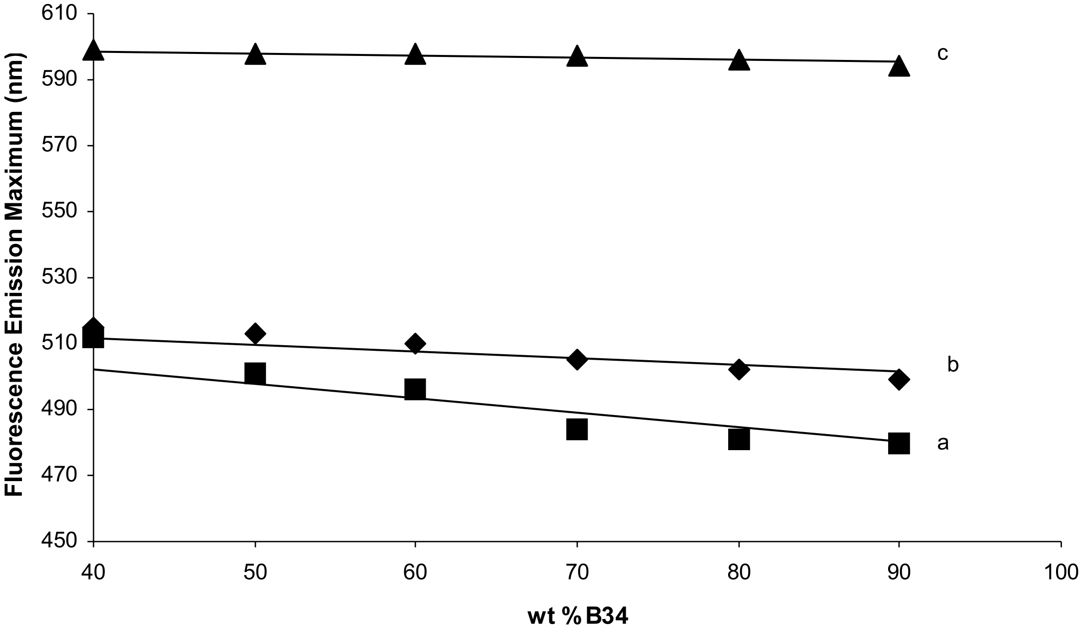

Fig. 6. Plot of fluorescence emission maxima vs. %B34 for the nanocomposites of (a) [1(CE-OPV):9EuCl$_3$]-B34 (b) (CE-OPV)-B34.

where the *d*-spacing change becomes the same, likely dominated by the PPV component of each molecule. Crown ether molecules alone were able to be intercalated, although the *d*-spacing change was much less than when attached to polymeric PPV chains, due to the latter's size and bulk. However, crown ethers alone are able to cause greater nanoclay layer separation than poly(ethylene oxide), even when the latter is of much higher molecular weight, no doubt due to the sterically bulky nature of the crown ether.

Fluorescence measurements of the nanocomposites show a steady decrease in emission maximum, as a function of amount of clay. A model is proposed in which the decrease in fluorescence emission wavelength is explained on the basis of partial intercalation. The fine color tuning as a function of intercalation, indicates the potential application of these materials in electro luminescent devices.

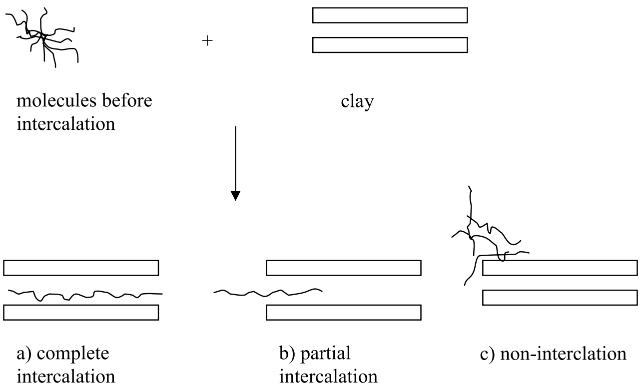

Scheme 2. Mechanism for intercalation of CE-OPV or EO-PPV into B34.

Acknowledgements

The authors would like to acknowledge the Australian Research Council for the Discovery grant provided for this project.

References

[1] Burroughes JH, Bradley DDC, Brown AR, Marks RN, Mackay K, Friend RH, et al. Nature 1990;347:539.
[2] Tessler N, Denton GJ, Friend RH. Nature 1996;382:695.
[3] Hide F, Diaz-Garcia MA, Schwartz BJ, Andersson MR, Pei Q, Heeger AJ. Science 1996;273:1833.
[4] Granstrom M, Petritsch K, Arias AC, Lux A, Anderson MR, Friend RH. Nature 1998;395:257.
[5] Pei Q, Yu G, Zhang C, Yang Y, Heeger AJ. Science 1995;269:1086.
[6] Pei Q, Yang Y, Yu G, Zhang C, Heeger AJ. J Am Chem Soc 1996; 118:3922.
[7] Sirringhaus H, Tessler N, Friend RH. Science 1998;280:1741.
[8] Narayan KS, Singh ThB. Appl Phys Lett 1999;74:3456.
[9] Halls JJM, Walsch CA, Greenham NC, Holmes AB, Marsegila EA, Friend RH, et al. Nature 1995;376:498.
[10] Kohler A, Dos Santos DA, Beljonne D, Shuai Z, Bredas JL, Holmes AB, et al. Nature 1998;392:903.
[11] Nazar LF, Zhang Z, Zinkweg D. J Am Chem Soc 1992;114:6239.
[12] Winkler B, Dai L, Mau AW-H. J Mater Sci Lett 1999;18:1539.
[13] Nguyen T-Q, Wu J, Doan V, Schwartz BJ, Tolbert SH. Science 2000; 288:652.
[14] Wu J, Gross AF, Tolbert SH. J Phys Chem B 1999;103:2374.
[15] Lee T-W, Park OO, Kim JJ, Hong J-M, Kim YC. Chem Mater 2001; 13:2217.
[16] Smith RC, Fischer WM, Gin DL. J Am Chem Soc 1997;119:4092.
[17] Yonesawa K, Gin DL. Polym Prepr 2000;41:1144.
[18] Johnson SA, Brigham ES, Olivier PJ, Mallouk TE. Chem Mater 1997; 9:2448.

[19] Yano K, Usuki A, Okada A. J Polym Sci, Part A: Polym Chem 1997;35:2289.
[20] Ramachandran K, Lerner MM. J Electrochem Soc 1997;144:3739.
[21] Carrado KA, Xu L. Chem Mater 1998;10:1440.
[22] Gowri R, Simon GP, Cheng YB, Smith TA, Dai L. J Fluoresc 2003;13:427.
[23] Winkler B, Mau AW-H, Dai L. Phys Chem Chem Phys 2000;2:291.
[24] Winkler B, Dai L, Mau AW-H. Chem Mater 1999;11:704.
[25] Gowri R, Mandal D, Shivkumar B, Ramakrishnan S. Macromolecules 1998;31:1819.
[26] Shen S, Simon GP, Cheng YB. Polymer 2002;43:4251.